https://doi.org/10.1007/s41230-020-9112-8

Thermal conductivity of cast iron – A review

Guang-hua Wang[1], *Yan-xiang Li[1, 2]

1. School of Materials Science and Engineering, Tsinghua University, Beijing 100084, China

2. Key Laboratory for Advanced Materials Processing Technology, Ministry of Education, Beijing 100084, China

Abstract: This paper gives a brief introduction to the four research methods for the study on thermal conductivity of cast irons, including experimental measurement, statistical analysis, effective medium theory and numerical simulation. Recent studies on the thermal conductivity of various cast irons are reviewed through the influence of alloying elements, structural constituents, and temperature. The addition of alloying elements is the main reason that restricts the thermal conductivity of cast irons, especially spheroidal graphite cast iron. The connectivity of graphite has a significant effect on the thermal conductivity of flake and compacted graphite cast irons, semi-quantitative and quantitative analysis of this factor is a key and difficult point in the study of thermal conductivity of cast irons. The thermal conductivities of different types of cast irons show varying degrees of dependence on temperature. This phenomenon is the combination of graphite and matrix, rather than just depending on graphite morphology. The study of the relationship between individual phase and temperature is the focus of future research. These summaries and discussions may provide reference and guidance for the future research and development of high thermal conductivity cast irons.

Key words: cast iron; thermal conductivity; gray cast iron; nodular cast iron; compacted graphite cast iron

CLC numbers: TG143; **Document code:** A; **Article ID:** 1672-6421(2020)02-085-11

***Yan-xiang Li**

Male, born in 1962, Ph.D. Tenure Professor in School of Materials Science & Engineering, Tsinghua University. He got his bachelor and master degrees in Harbin Institute of Technology in 1982 and 1985, and Ph.D in Tsinghua University in 1989. His research interests are mainly focused on casting alloys (cast irons, cast steels, and cast nonferrous metals as aluminium), porous metals (aluminium foams and lotus-type metals); and solidification process, especially directional solidification of alloys. He has published over two hundred papers in international and domestic journals, and dozens of conference reports. He is now the Chairman of the WFO Ferrous Metals Commission and a member of the Foundry Institution of Chinese Mechanical Engineering Society.

E-mail: yanxiang@tsinghua.edu.cn

Received: 2019-10-08

Accepted: 2019-11-20

Cast irons are among the most widely used metallic materials due to their good mechanical and physical properties, excellent casting ability and low cost. According to the survey of Modern Casting [1], as shown in Fig. 1, outputs of lamellar graphite cast iron (LGI) are much higher than that of spheroidal graphite cast iron (SGI) though SGI has better mechanical properties. One of the reasons is that LGI has wide applications at high temperatures due to its superior thermal conductivity. That's why the LGI and compacted graphite cast iron (CGI) are widely applied in brake disc, engine block and cylinder head [2-5]. The thermal conductivity is an extremely important performance index for cast irons. The high thermal conductivity can help to transfer heat rapidly and prevent thermo-mechanical fatigue, deformation and hot cracking, thereby ensuring the applications of cast irons in more complex or harsher conditions and improving the service life of products [6]. Therefore, on the premise of basic mechanical properties, the design and development of high thermal conductivity cast irons is one of the key points in the research and development of cast irons.

Cast irons are multi-component alloys with regular elements of C and Si and some commonly added alloying elements, such as Mn, Cu, Ni, Cr, W, Mo, V, Ti, Al, etc. The microstructure of cast irons is complicated, usually composed of ferrite, pearlite, graphite, and cementite. So, the thermal conductivity of cast irons is dependent on both the alloying elements and structural constituents.

During solidification, the formation of cast iron microstructure, especially the graphite morphology, is governed by the difference in thermal conductivity between graphite and austenite in eutectic couple, and between different orientations of graphite crystals [7]. According to different graphite morphologies, cast irons where carbon precipitated in the form of graphite (graphite cast irons) are mainly divided into LGI with lamellar graphite, CGI with compacted graphite and SGI with spheroidal graphite. Generally, the thermal

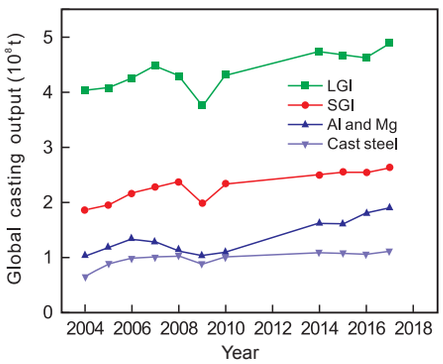

Fig. 1: Census of world casting production [1]

conductivity of LGI is the highest, and that of SGI is the lowest. With an intermediate form of graphite, CGI has a thermal conductivity between that of LGI and SGI [8]. The ranges of thermal conductivity for the three types of cast irons are shown in Table 1.

Table 1: Thermal conductivities of three types of cast irons at 300 K

Type	Thermal conductivity ($W \cdot m^{-1} \cdot K^{-1}$)
LGI	45–60
CGI	32–45
SGI	25–40

The thermal conductivity k is defined as

$$k = -q/\nabla T \quad (1)$$

where q is the heat flux, ∇T is the temperature gradient.

Heat energy is transmitted through various carriers, such as electrons, phonons and photons. In metals, electrons carry the majority of the heat, but the contribution of phonons cannot be neglected, especially in iron-based alloys [9-11]. The total thermal conductivity of a metal is

$$k = k_p + k_e \quad (2)$$

where k_p and k_e are phonon and electron thermal conductivity, respectively.

The thermal conductivity of cast irons is limited by various scattering processes. Over 300 K, phonon scattering processes of iron-based alloys mainly include phonon-phonon scattering, phonon-impurity scattering and phonon-electron scattering. The electron scattering processes mainly include electron-phonon scattering and electron-impurity scattering. Therefore, the thermal conductivity is determined by impurities, dislocations, grain boundary defects and conducting electrons and phonons [8,10,11]. These scattering mechanisms of cast irons are mainly affected by alloying elements, structural constituents and temperature.

At present, research methods on the thermal conductivity of cast irons are mainly divided into experimental measurement, statistical analysis, effective medium theory (EMT) and numerical simulation. In the early days, experimental methods were usually used to study the thermal conductivity of cast irons. Because there are many uncontrollable factors in experiments, such as chemical composition, process parameters, it is difficult to control a single variable, which leads to dispersed experimental results. In recent years, some researchers studied influencing factors on the thermal conductivity of cast irons by means of statistical analysis [12-15] and machine training [16]. These methods require a large amount of data which determines the accuracy of calculation results. Because graphite cast irons can be regarded as composite materials composed of the matrix and different types of graphites, the overall thermal conductivity can be obtained from the thermal conductivity of each constituent phase based on the EMT [17,18]. The accuracy of this method only depends on the values of each constituent phase, thus greatly reducing the time of experiments. However, the position, size, orientation, and shape of reinforcing particles need to be taken into account in the EMT [19]. At present, simplifications of various types of graphites can hardly reflect true 3-D graphite morphologies in graphite cast irons [18, 20, 21]. With the development of numerical simulation, it is possible to directly input real microstructures obtained from experiments into the simulation software to obtain properties of macroscopic materials [20]. In recent years, some researchers have attempted to simulate 2-D or 3-D structures of graphite cast irons obtained by experiments [2,20,21], so as to evaluate the thermal conductivity of graphite cast irons. However, there are still unexpected deviations between calculated results and experimental data.

In this paper, firstly, the four research methods for thermal conductivity of cast irons were introduced. Then, recent studies on the thermal conductivity of various cast irons are reviewed from the aspects of alloying elements, structural constituents and temperature. It is expected that these works can provide reference and guidance for the future research and development of high thermal conductivity cast irons.

1 Research methods

1.1 Experimental measurement

Methods for measuring the thermal conductivity of materials are mainly divided into steady state methods and transient methods. Steady state methods include calorimeter flow method, hot plate method and longitudinal heat flow method, etc [22]. Their principle is to use heat source to heat the sample and reach a thermal equilibrium state. Therefore, a stable temperature field will be formed inside the sample. According to the temperature gradient and the heat transfer rate per unit area, the thermal conductivity of the material is obtained based on Eq. (1) [23]. The steady state method has advantages of clear principle, accurate and direct acquisition of the absolute value of thermal conductivity. But it is primitive, time-consuming and high environment demanding (such as adiabatic condition of measuring system, strict temperature control, shape and size of sample) [24].

Transient methods include hotline method [25], hot disk method [26] and flash method [27]. For a transient method, the temperature distribution in the sample varies with time, so a stable temperature

field cannot be formed. The thermal diffusivity of the sample can be determined by measuring the temperature change rate of the sample surface, and the thermal conductivity of the sample can be obtained indirectly [23]. The relationship between thermal conductivity and thermal diffusivity satisfies

$$k=\rho a c_p \tag{3}$$

where ρ is the density, a is the thermal diffusivity and c_p is the specific heat capacity.

Flash method is the most widely used transient method for measuring thermal diffusivity of materials because of short measuring period, wide temperature ranges and high accuracy. For cast irons, the thermal conductivity was obtained by flash method in most literatures [8,12-16,28]. The thermal diffusivity can be calculated by [27]

$$a=\frac{0.1388l^2}{t_{0.5}} \tag{4}$$

where l is the specimen thickness and $t_{0.5}$ is the time required to reach half of temperature rise.

Because there are many uncontrollable factors in experiments, such as chemical composition, process parameters, it is difficult to control a single variable, which leads to dispersed experimental data. There are many factors affecting the thermal conductivity of cast irons. It is blindness to develop high thermal conductivity cast irons by trial-and-error method, which takes a long experimental period to obtain expected results.

1.2 Statistical analysis

Statistical analysis is used to establish the relationship between thermal conductivity and main parameters of cast irons based on a large number of experimental data. Holmgren et al. [12] established a linear regression model for the thermal conductivity of pearlitic CGI and SGI based on nodularity N and cementite fraction f_γ:

$$k=a_T+N\times b_T+f_\gamma\times c_T \tag{5}$$

where $a_T=-5\times10^{-5}T^2+0.0271T+35.449$, $b_T=9\times10^{-5}T-0.127$, and $c_T=4\times10^{-7}T^2+0.0002T-0.343$, T is temperature (°C). Calculated results are in good agreement with experimental data.

Subsequent experimental study shows that the contents of C and Si also have a significant effect on the thermal conductivity of cast irons [13]. For the pearlitic CGI and SGI, a modified linear regression model was established by considering four parameters: C content, Si content, nodularity N and cementite fraction f_γ:

$$k=a_T+\mathrm{C}\times b_T+\mathrm{Si}\times c_T+N\times d_T+f_\gamma\times e_T \tag{6}$$

Selin et al. [14] introduced ferrite fraction in the matrix, f_α, and established a linear regression analysis equation for the thermal conductivity of CGI based on 76 experimental data. The calculated results are in good agreement with experimental results of Holmgren et al. [12] and Dawson [29]. Jalava et al. [15] made a polynomial regression model for SGI based on temperature, Si content and pearlite fraction in matrix:

$$k=72.56+0.06721x_1-21.67x_2-0.2458x_3-0.000161x_1^2+2.173x_2^2+0.00414x_1x_2+0.0541x_2x_3 \tag{7}$$

where x_1=temperature (°C), x_2=silicon (%), x_3=pearlite (%). Estimated values from the model matched quite closely to actual measured values.

Wang et al. [16] established an adaptive neuro-fuzzy inference system to link the thermal conductivity and related parameters of LGI, consisting of graphite content, maximum graphite length, primary dendrite percentage and hardness of the matrix. This nonlinear machine training model provides a good prediction on the basis of the experimental measurements; it is more accurate than traditional linear regression models.

The parameters in these statistical analyses are usually easy to obtain based on experimental data, and require no assumptions such as the thermal conductivity of each constituent phase. But, if the data set is too small or narrow, the model will not be as general and useful [14].

1.3 Effective medium theory

In order to study the macroscopic properties of composites, it is assumed that a single-phase medium, and its properties can be equivalent to those of composites as a whole. This theory is called the EMT. It was first proposed by Maxwell [30] based on the electric potential satisfying Laplace equation to calculate the effective electrical resistivity of spherical particle composites. Eucken [31] developed Maxwell's model to describe the thermal conductivity of particle reinforced composites by analogizing the electric potential field with the temperature field. The model is shown in Fig. 2 [32]. And the corresponding expression is

$$k_{\mathrm{eff}}=\frac{2k_\mathrm{m}+k_\mathrm{d}+2f(k_\mathrm{d}-k_\mathrm{m})}{2k_\mathrm{m}+k_\mathrm{d}-f(k_\mathrm{d}-k_\mathrm{m})}k_\mathrm{m} \tag{8}$$

where k_{eff} is the effective thermal conductivity, k_m is the thermal conductivity of matrix, k_d is the thermal conductivity of reinforcement phase, f is the volume fraction of reinforcement phase.

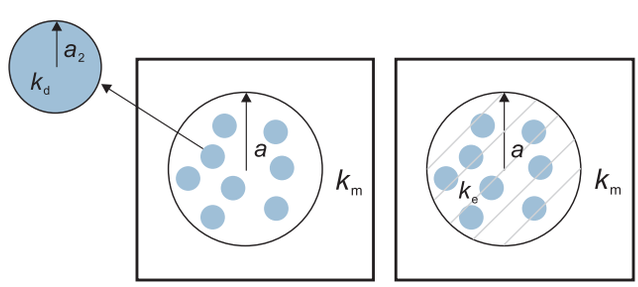

Fig. 2: Illustration of Maxwell's modeling to the effective thermal conductivity of a heterogeneous sphere containing spherical particles [32]

With the development of EMT, it can be used to calculate the thermal conductivities of composites with higher volume fraction [33], anisotropic distribution [34], interfacial thermal resistance [34,35], and reinforcing phases of various shapes [34,36,37].

Because graphite cast irons could be regarded as in-situ

composite materials consisting of matrix and different types of graphites, Helsing et al. [18] established the thermal conductivity of LGI and SGI based on mean field approximation. The effective thermal conductivity of SGI, k_S, is

$$k_s=k_m+f(\frac{3}{2+\eta k_c/k_S})\times(\frac{2k_a+\eta k_c}{2+\eta}-k_m)+3f_\gamma k_S\frac{k_\gamma k_m}{2k_S+k_\gamma} \quad (9)$$

The effective thermal conductivity of LGI, k_L, is [18]

$$k_L=k_m+\frac{1}{3}fk_L(\frac{k_c-k_L}{k_L+L_{33}(k_c-k_L)}+2\frac{k_a-k_m}{k_L+L_{11}(k_a-k_L)})+3f_\gamma k_L\frac{k_\gamma-k_m}{2k_L+k_\gamma} \quad (10)$$

where k_m is the effective thermal conductivity of matrix (matrix can be ferrite or/and pearlite), k_γ is the thermal conductivity of cementite, k_a is the thermal conductivity of graphite in-plane, k_c is the thermal conductivity of graphite cross-plane, f is the volume fraction of graphite, f_γ is the volume fraction of cementite, $\eta=\frac{1}{2}[(1+8k_a/k_c)^{1/2}-1]$, $L_{11}=\frac{p^2}{2(p^2-1)}+\frac{p}{2(1-p^2)^{3/2}}\cos^{-1}p$ $(p<1)$, $L_{33}=1-2L_{11}$, p is the aspect ratio.

The accuracy of EMT model depends not on the amount of experimental data, but on the values of parameters and simplification of the model. It can be flexibly applied to cast irons with various graphite morphologies and microstructures [14]. Therefore, it has been widely used in recent years [38-40,84]. However, interconnected structures with lamellar and compacted graphite are not considered in these models, and the results are independent of graphite size. It is not consistent with the real situation.

Velichko et al. [20] calculated the upper and lower boundaries for thermal conductivity of various types of cast irons based on rule of mixture and Hashin-Shtrikma model, and compared them with experimental data. Results showed that the thermal conductivity of LGI and CGI mainly depended on the thermal conductivity of graphite in-plane, while that of SGI mainly depended on the thermal conductivity of matrix [20]. Matsushita et al. [40] calculated the thermal conductivity of CGI and SGI based on various EMT models, and evaluated the prediction accuracy of each model. Calculated results showed that the thermal conductivity could be estimated by using Helsing model. The Maxwell's model [30], Bruggeman's model [33] and Hashin-Shtrikman model [41] were also applicable with the thermal conductivity of graphite in-plane.

Although the EMT has been widely used in the calculation for thermal conductivity of composite materials, there are still many problems in the application of this theory to the study on thermal conductivity of cast irons. The accuracy of a model calculation depends on parameters, but there is no reliable values of matrix and graphite thermal conductivity for cast irons with different compositions. The 3-D morphologies of graphite are very complex. For example, graphite in a eutectic cell of LGI and CGI is interconnected. At present, no physical models reported can reflect the actual morphologies of graphites in cast irons [18,20,21].

1.4 Numerical simulation

Numerical simulation can be used to shorten the material development cycle effectively, but the application of this technology in cast irons is not so mature because main intensive studies of cast irons are much earlier than the emergence of numerical simulation [21]. Because cast iron is considered as a structural material, simulations of cast irons in the past were mainly focused on the microstructure formation [42-45] during solidification process and mechanical behavior [46-48], those on thermal conductivity are rarely reported.

Velichko et al. [20,49] used focused ion beam (FIB) tomography to analyze the 3-D morphologies of different types of graphites. Then, 3-D simulation on real tomographic data was carried out. The results showed that graphite connectivity was one of the determining factors for the thermal conductivity of cast irons [20]. According to metallographic pictures, Ma et al. [2] calculated the effective thermal conductivity of CGI based on finite element method. But the 2-D simulation results were far from the experimental data. The author attributed to the interfacial thermal resistance (ITR) between graphite and matrix, but the value of ITR in composites is much higher than the author's hypothesis [50,51]. Then, the 3-D finite element model of CGI was established by X-ray computed tomography. The simulation suggested that the connectivity of graphite in CGI can improve its thermal conductivity [21]. Yang et al. [52] built a 2-D finite element model for thermal conductivity of the metallographic microstructure of oxidized CGI. The simulation results showed that with the increase of oxide layer thickness, the heat transfer efficiency of graphite decreased, and that of the matrix became gradually dominant.

The numerical simulation can be used to directly input real microstructures obtained from experiments into the simulation software to obtain thermal conductivities of cast irons, and deal with complex 3-D graphite morphologies of cast irons. However, the application of this technology to the thermal conductivity of cast irons is not so mature yet, there are still unexpected deviations between calculated results and experimental data [2,20,21,52]. Moreover, a large number of simulation examples are needed to obtain the corresponding numerical solutions of different parameter values. Therefore, this method is not very suitable for the study of influencing factors compared with the EMT.

2 Effect of alloying elements

Because the thermal conductivity of graphite in-plane is much higher than that of matrix, the thermal conductivity of cast irons was increased by improving the graphite morphology in the past. Corresponding research was mainly focused on the influence of graphite parameters on the thermal conductivity of cast irons, such as graphite morphology, graphite volume fraction and graphite growth direction. The addition of alloying elements has always been used to improve the mechanical properties of cast irons. In fact, the relationship between mechanical properties and thermal conductivity is often opposite [16, 53, 54, 85]. The addition of alloying elements often reduces the thermal conductivity of cast irons. One of the key reasons is that the addition of alloying

elements reduces the thermal conductivity of matrix, which is an important part of cast iron structural constituents, and then reduces the thermal conductivity of cast iron [10].

According to Williams et al. [55,56], the thermal conductivity of pure ferrite at 300 K was about 78.6 $W \cdot m^{-1} \cdot K^{-1}$. With the addition of alloying elements, the solid-soluble alloying elements in the ferrite scattered phonons and electrons, increasing the electrical resistivity and lattice thermal resistance of alloyed ferrite, thus greatly reducing the thermal conductivity of ferrite. Helsing et al. [18] proposed an equation to calculate the thermal conductivity of alloyed ferrite at 300 K:

$$k_\alpha=\left(\frac{\rho_{Fe}}{LT}+\frac{\rho_{Fe}}{L_0T}\sum_i\rho_i'c_i\right)^{-1}+[k_p^{-1}(Fe)+\sum_i A_i c_i]^{-1} \quad (11)$$

where ρ_{Fe} and k_p (Fe) are the electrical resistivity and phonon thermal conductivity of pure ferrite, respectively. ρ_i' and A_i are contribution coefficients to electrical resistivity and lattice thermal resistance for alloying element i, respectively. c_i is the atomic fraction of alloying element i, L is the Lorentz number and L_0 is the Lorentz constant. T is temperature (K). The parameters of some alloying elements are given in Table 2.

The deviations of lattice thermal resistance contribution coefficients calculated from different literature are great due to measurement errors. Based on the theory of metal heat conduction, Eq. (11) was further revised [10]:

$$k_\alpha=\frac{1}{1.61\times10^{-2}+1.36\times10^{-3}\sum_i\rho_i'c_i}+\frac{1}{5.65\times10^{-2}+1.36\times10^{-2}\sum_i c_i\Gamma_i} \quad (12)$$

where Γ_i is the impurity scattering parameter, and the Γ_i values of some alloying elements are listed in Table 2.

Table 2: Experimental values for coefficients ρ_i' and A_i, and calculated Γ_i values of some elements at 300 K [10, 18]

	Al	Sn	Si	Cr	Mn	Ni	Mo	W	Co	Cu
ρ_i' [μΩ·cm·(at.%)$^{-1}$]	6.4	10.0	7.0	4.6	5.0	2.7	4.8	5.0	1.1	3.2*
$A_i\times10^3$[m·K·W^{-1}·(at.%)$^{-1}$]	7.0	-	8.0	0.1	10.0	4.0	13.0	40.0	-	-
Γ_i [m·K·W^{-1}·(at.%)$^{-1}$]	0.1	12.0	0.6	0	0	0	1.7	8.5	-	0

*The coefficient ρ_i' of Cu is derived from Ref. [62].

The relationships between the thermal conductivity of ferrite and some alloying elements calculated by Eq. (12) are shown in Fig. 3. It can be seen that all alloying elements significantly reduce the thermal conductivity of ferrite. Effects of Si and Al on the thermal conductivity of ferrite are strong, and the effect of W is weak. Effects of Mn, Cr and Mo are similar and medium. However, with the addition of 3wt.% Si, effect of W is stronger than that of Mn. This result shows that the superposition of another element may change the influence of an alloying element on the thermal conductivity of ferrite [10]. Terada et al. [57] systematically studied the thermal conductivities of 22 groups of ferrous binary alloys. The experimental results demonstrated that the addition of alloying elements always reduced the thermal conductivity of ferrite.

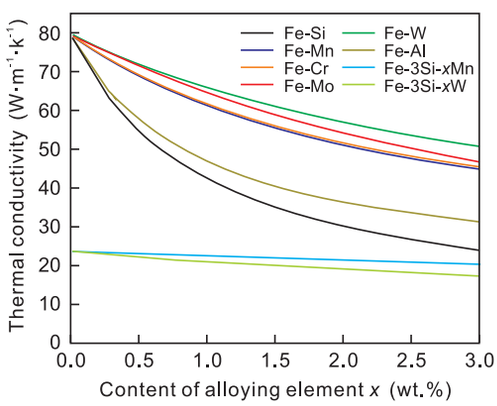

Fig. 3: Relationship between the thermal conductivity of iron-based alloy and contents of alloying elements at 300 K [10]

For graphite cast irons, alloying elements not only dissolve in ferrite, but also have a significant effect on the microstructure. For example, carbide-forming elements such as V, Cr, Mo, W, Mn form low thermal conductivity carbides with carbon [58]. Cu, Ni, and Sn will strongly promote the formation of pearlite [83]. Al and Si promote the formation of ferrite and graphite, but their solid solution greatly reduces the thermal conductivity of ferrite [58,59]. The results of Rukadikar et al. [58] and Ding et al. [60] confirmed that the thermal conductivity of LGI could be improved by adding Mo. One of the reasons is that Mo element may increase the total length of flake graphite, thus improving the thermal conductivity of gray cast iron [60]. However, the experimental results of Xu et al. [61] show that Mo will reduce the thermal conductivity of CGI.

In summary, almost all alloying elements reduce the thermal conductivity of cast irons. One of the key reasons is that solid-soluble alloying elements scatter phonons and electrons of ferrite and therefore reduce the thermal conductivity. Of course, the addition of alloying elements also has a significant impact on the microstructure, such as the formation of carbides, promotion of pearlite and graphite, and improvement of graphite morphologies, thereby affecting the thermal conductivities of cast irons.

3 Effect of structural constituents

The structure of graphite cast irons is mainly composed of the matrix and graphite. The matrix includes ferrite, pearlite, cementite and so on. Table 3 gives the values of thermal

conductivity of each constituent of cast irons at 300 K. The thermal conductivity of graphite is strongly anisotropic. The thermal conductivity of graphite in-plane is much greater than that of graphite cross-plane because of the large lattice spacing and weak bonding force between basal planes. At 300 K, the ideal thermal conductivity of graphite in-plane k_a reaches 2,000 $W \cdot m^{-1} \cdot K^{-1}$ [68], but in fact, k_a of different kinds of graphite has an extraordinary wide span, as listed in Table 4. For the pyrolytic graphite, the crystal structure is highly regular with few defects, and the thermal conductivity can approach 2,000 $W \cdot m^{-1} \cdot K^{-1}$ in theory [64,67]. The polycrystalline graphite is aggregated from a large number of grains with different orientations. It is scattered by grain boundaries, defects and sample boundaries [67]. So the measured values are only 100–500 $W \cdot m^{-1} \cdot K^{-1}$ [63,64].

Table 3: Thermal conductivities of structural constituents of cast iron at 300 K

Structural constituent	Thermal conductivity ($W \cdot m^{-1} \cdot K^{-1}$)	Ref.
Graphite in-plane	1,950	[64]
Graphite cross-plane	5.7	[64]
Pure ferrite	80	[56, 65, 66]
Alloyed ferrite	20–40	[8]
Cementite	8	[12, 18, 38]
Pearlite	17–36	[8,18]

Table 4: Thermal conductivities of graphites at 300 K

Graphite	In-plane ($W \cdot m^{-1} \cdot K^{-1}$)	Cross-plane ($W \cdot m^{-1} \cdot K^{-1}$)	Ref.
Acheson graphite [a]	165	119	[64]
AGOT graphite [a]	220	138	[64, 67]
Pyrolytic graphite	1,950	5.7	[40, 64, 67]
Calculated intrinsic value	1,910	–	[68]
Graphite of cast iron [b]	293–419	84	[8, 63]
Graphite of cast iron	500	10	[18, 20]
Graphite of cast iron	800	10	[38]

[a] The thermal conductivity of Acheson and AGOT graphite in-plane is taken from that of graphite parallel to extrusion axis. The thermal conductivity of Acheson and AGOT graphite cross-plane is taken from that of graphite vertical to extrusion axis. [b] Measured temperature is between 273–373 K.

For cast irons, as graphite is crystallized from melt, its lattice perfection is much better than that of ordinary polycrystalline graphite. Therefore, it is considered that k_a and k_c are close to 1,950 $W \cdot m^{-1} \cdot K^{-1}$ and 5.7 $W \cdot m^{-1} \cdot K^{-1}$, respectively. The thermal conductivity of pure ferrite k_{Fe} is about 80 $W \cdot m^{-1} \cdot K^{-1}$ [56,65,66], but that of alloyed ferrite in various cast irons calculated by Eq. (12) is almost 20–40 $W \cdot m^{-1} \cdot K^{-1}$ according to the data in Ref. [8]. This indicates that effects of alloying elements on the thermal conductivity of ferrite are significant. The thermal conductivity of cementite k_γ is about 8 $W \cdot m^{-1} \cdot K^{-1}$ [18,38]. The effective thermal conductivity of lamellar pearlite can be calculated according to Helsing's formula [18]

$$k_\beta = \frac{1}{4}[k_\beta^{\parallel} + (k_\beta^{\parallel 2} + 8k_\beta^{\parallel}k_\beta^{\perp})^{1/2}] \quad (13)$$

where $k_\beta^{\parallel} = f_\alpha k_\alpha + f_\gamma k_\gamma$, $k_\beta^{\perp} = (f_\alpha/k_\alpha + f_\gamma/k_\gamma)^{-1}$. The effective thermal conductivity of pearlite calculated by Eq. (13) is 17–36 $W \cdot m^{-1} \cdot K^{-1}$.

At present, the relationship between structural constituents and thermal conductivity of cast irons was reported extensively. The parameters related to the matrix mainly include pearlite fraction [8,14,15] and carbide content [14]. The parameters related to graphite include graphite morphology such as graphite length, aspect ratio and roundness coefficient [8,16,18,20,38,40], graphite volume fraction [16], nodularity or vermicularity [2,8,12-14,69], graphite growth direction [70]. However, few studies have been reported about the effect of graphite connectivity on the thermal conductivity of cast irons.

Buning et al. [71] considered that graphite in each eutectic cell was connected with each other after polishing and corrosion of cast iron specimens containing rough flake graphite layer by layer. During 1970s–1980s, with the development of SEM and its application in cast iron research, SEM was used to observe deep etched specimens of cast irons, revealing the 3-D morphological characteristics of different types of graphites. Results verified that lamellar and compacted graphites are interconnected in each eutectic cell [72-75]. But the study about the effect of graphite connectivity on the thermal conductivity of cast irons is just a simple qualitative analysis. With the development of X-ray computed tomography and numerical simulation, semi-quantitative or quantitative analysis of the relationship between graphite connectivity and thermal conductivity of cast iron becomes possible.

The 3-D morphologies of flake and compacted graphites are shown in Figs. 4 and 5. It is obvious that graphite is interconnected in the reconstructed 3-D structure. Velichko et al. [20,76] visualized and studied complex graphite morphologies and quantitatively characterized their geometry, shape and connectivity. Corresponding 3-D numerical simulation results proved that the connectivity of graphite was one of

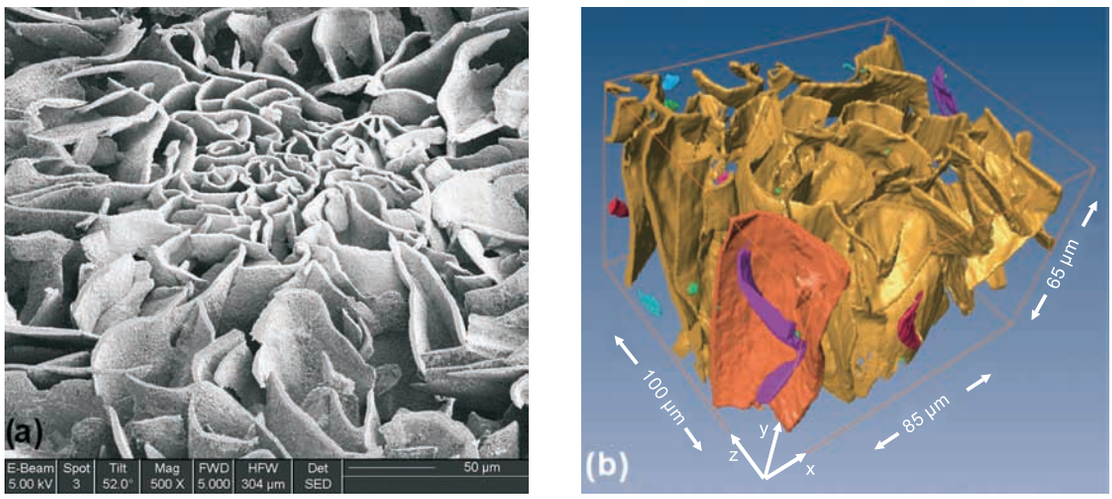

Fig. 4: (a) SEM image of flake graphite, deep etched; (b) Reconstructed 3-D structure of flake graphite based on Focused Ion Beam (FIB) tomography [49]

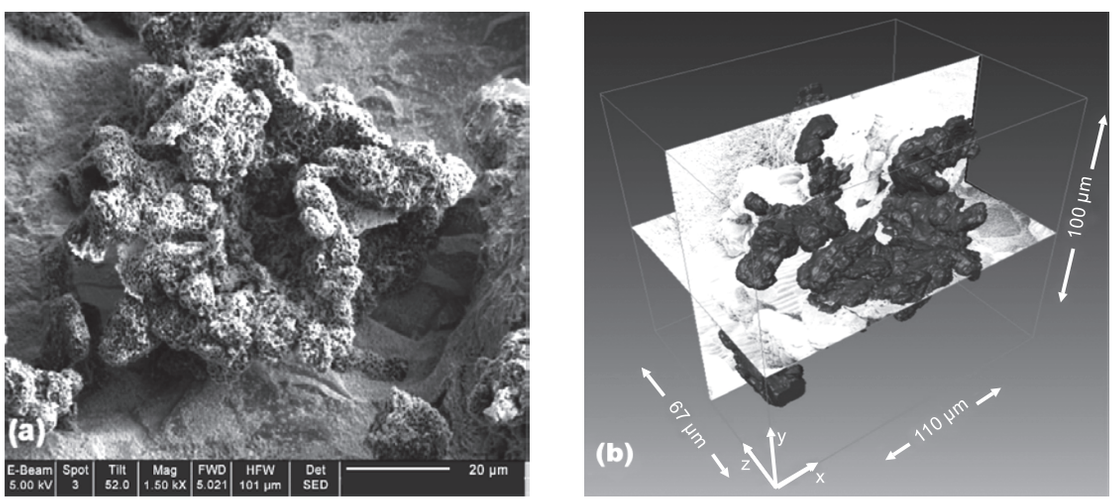

Fig. 5: (a) SEM image of compacted graphite, deep etched; (b) Reconstructed 3-D structure of compacted graphite based on Focused Ion Beam (FIB) tomography [49]

the determining factors for the thermal conductivity of cast irons. Yang et al. [77] studied the solidification process and microstructure evolution of eutectic gray cast iron by using digital optical microscopy and high resolution X-ray diffraction methods. The results showed that the connectivity of graphite increased with the crystallization process, and the connectivity of graphite was about 88.87% at the end of eutectic reaction. Ma et al. [21] constructed 2-D and 3-D finite element models of CGI in the same way, and calculated the thermal conductivity by using finite element software ANSYS. The simulation showed that the thermal conductivity of CGI with 40% vermicularity was 7.4% higher than that of 2-D model, which indicated that the connectivity of graphite had a promoting effect on the thermal conductivity of CGI.

In this section, the thermal conductivities of each structural constituent in cast irons at 300 K are given based on a large number of data. Although there are many studies on the relationships between structural constituents and thermal conductivity of cast irons, the effect of graphite connectivity on thermal conductivity has rarely been reported. Deep etch and X-ray tomography show that flake graphite and compacted graphite are interconnected in each eutectic cell, but the effect of graphite connectivity on the thermal conductivity of cast iron is still not clear.

4 Effect of temperature

A large number of previous works show that the thermal conductivity of various cast irons also depends on temperature [8,12-15,38,55,61,66,69,70,78]. Figure 6 shows the typical curves of thermal conductivity for various cast irons with temperature [70]. It can be seen that the thermal conductivity of LGI has the strongest dependence on temperature and decreases monotonously with the increase of temperature, while the thermal conductivities of CGI and SGI have relatively small dependence on temperature. It increases first and then decreases slightly with the increase of temperature. The peak value temperature of CGI is usually between 200 and 300 °C, and the peak value temperature of SGI is often higher, even there is no peak value temperature in the temperature range of 300–

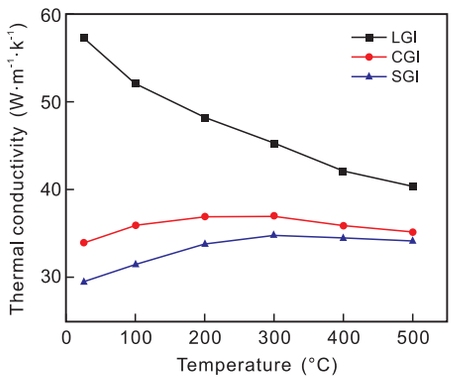

Fig. 6: Relationship between thermal conductivities of various cast irons and temperature [70]

800 K [78]. Although presently there are many reports about the effect of temperature on the thermal conductivity of cast irons, the explanation of this phenomenon is not clear. This phenomenon is the result of combination action of matrix and graphite. Therefore, the influence of temperature on the thermal conductivity of cast iron depends on the relationship between each constituent phase and temperature.

For the ferrite, the experimental results of Williams et al. [55] and Terada et al. [57] showed that the thermal conductivity of pure ferrite decreased monotonously with the increase of temperature. With the addition of alloying elements, the thermal conductivity of alloyed ferrite increased at first, then decreased, at last increased monotonously. Similar phenomena also exists in alloyed steels [79,80]. The reason is that although the phonon thermal conductivity decreases monotonously with the increase of temperature, the relationship between electron thermal resistance and temperature changes from monotonic decrease to monotonic increase with the increase of contents of alloying elements [10], as shown in Fig. 7.

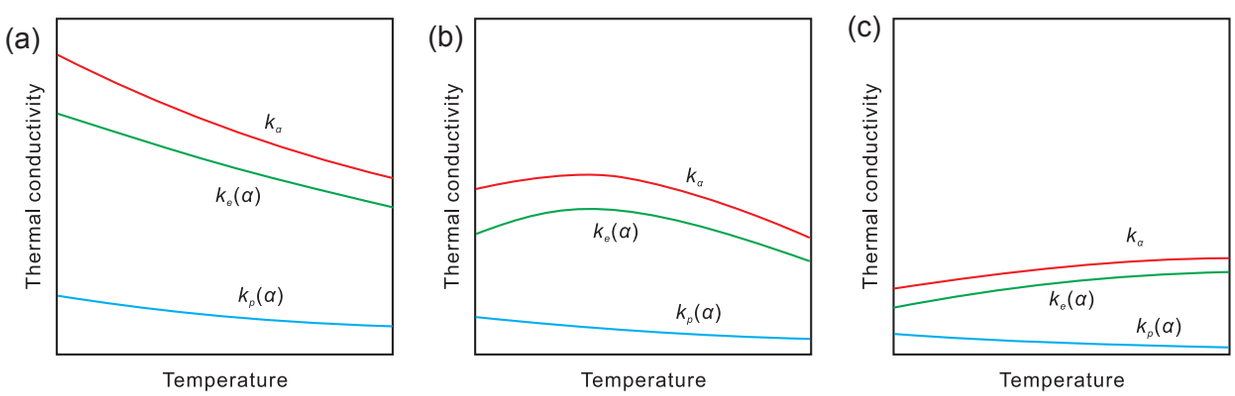

Fig. 7: Schematic diagram of relationship between thermal conductivity of alloyed ferrite and temperature at low (a), medium (b), and high (c) alloying content [10]

Figure 8 shows the relationship between the thermal conductivity of pyrolytic graphite and temperature [64]. It can be seen that the thermal conductivity of graphite both in-plane and cross-plane decreases monotonously with the increase of temperature during 300–800 K. Klemens [81,82] calculated the phonon thermal conductivity of graphite in the basal plane of single crystals at room and at elevated temperatures:

$$k_a=57300/T \quad (14)$$

where T is temperature (K). According to solid physics, for phonon scattering, at $T > \theta_D$, the contribution to thermal resistance W is given by [11]

$$W=AT/\theta_D \quad (15)$$

where A is a constant and calculated by the Liebfried-Schlmann equation modified by Julian [81], θ_D is the Debye temperature. When $T > \theta_D$, the phonon thermal conductivity is approximately inversely proportional to temperature. Therefore, the relationship between the thermal conductivities of various graphites in cast irons and temperature approximately satisfies

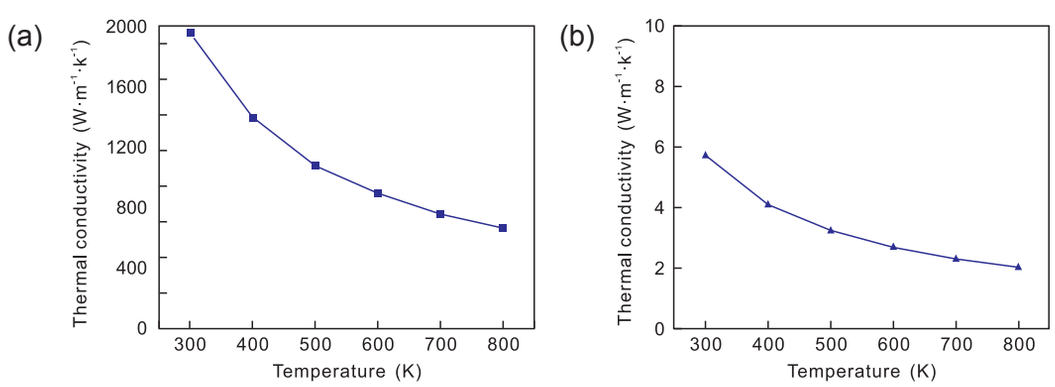

Fig. 8: Thermal conductivity of pyrolytic graphite: (a) in-plane; (b) cross plane [64]

inverse proportion.

Combining with Figs. 6–8, it can be seen that the relationship between the thermal conductivities of CGI and SGI and temperature is similar to that of high content alloyed ferrite, while that of LGI is similar to graphite and pure ferrite. It is suggested that the dependence of thermal conductivity of LGI on temperature mainly depends on graphite and ferrite, while that of CGI and SGI mainly depends on the content of alloying elements in the matrix. The relationship between thermal conductivity of various cast irons and temperature is the result of the combination of matrix and graphite.

5 Summaries

The research methods for the study on thermal conductivity of cast iron are summarized. Recent studies on the thermal conductivity of various cast irons are reviewed through the influence of alloying elements, structural constituents and temperature.

(1) In the early days, studies on the thermal conductivity of cast iron always used experimental methods. But it is difficult to control a single variable, which leads to dispersed experimental data. Statistical analysis can determine the influencing factors by solving the main parameters which affect the thermal conductivity of cast irons based on the experimental data, but the accuracy of the model depends on a large number of data. The effective medium theory has been widely used in the calculation for thermal conductivity of composite materials, but there are still many problems in the application of this theory to the study of thermal conductivity of cast irons such as the simplification of complex 3-D graphite morphologies. Numerical simulation can be used to deal with complex microstructure, but the application of this technology to the thermal conductivity of cast iron is not mature yet.

(2) Almost all alloying elements reduce the thermal conductivity of cast irons. One of the key reasons is that solid-soluble alloying elements scatter phonons and electrons of ferrite, which reduces the thermal conductivity. The addition of alloying elements also has a significant influence on the microstructure, such as the formation of carbides, promotion of pearlite and graphite, and improvement of graphite morphologies, thereby affecting the thermal conductivity of cast irons. The addition of alloying elements is the main reason that restricts the thermal conductivity of cast irons, especially spheroidal graphite cast iron.

(3) The connectivity of graphite has a significant effect on the thermal conductivities of flake and compacted graphite cast irons, but the corresponding research is not deep enough. Therefore, semi-quantitative and quantitative analysis of this factor is a key and difficult point in the study of thermal conductivity of cast irons.

(4) The thermal conductivities of different types of cast irons depend on temperature differently. The thermal conductivity of flake graphite cast iron decreases monotonously with the increase of temperature, just like that of graphite and pure ferrite. That of compacted and spheroidal graphite cast irons increases first and then decreases, just like that of alloyed ferrite depending on the content of alloying elements. This phenomenon is the combination of graphite and matrix, rather than just depending on graphite morphology. The study of the relationship between individual phase and temperature is the focus of future research.

Acknowledgements

The authors gratefully acknowledge the financial support by the National Natural Science Foundation of China (Grant No. 51371104).

References

[1] Census of world casting production: 2004-2017, Modern Casting. http://www.thewfo.com/census/ [17/7/2019].
[2] Ma Z J, Tao D, Yang Z, et al. The effect of vermicularity on the thermal conductivity of vermicular graphite cast iron. Materials & Design, 2016, 93: 418–422.
[3] Pevec M, Oder G, Potrč I, et al. Elevated temperature low cycle fatigue of grey cast iron used for automotive brake discs. Engineering Failure Analysis, 2014, 42: 221–230.
[4] Bagnoli F, Dolce F, Bernabei M, et al. Thermal fatigue cracks of fire fighting vehicles gray iron brake discs. Engineering Failure Analysis, 2009, 16(1): 152–163.
[5] Lan P, Zhang J Q. Strength, microstructure and chemistry of ingot mould grey iron after different cycles of low frequency high temperature loads. Materials & Design, 2014, 54(1): 112–120.
[6] Witik R A, Payet J, Michaud V, et al. Assessing the life cycle costs and environmental performance of lightweight materials in automobile applications. Composites, Part A: Applied Science and Manufacturing, 2011, 42(11): 1694–1709.
[7] Li Y X, Liu B C, Loper Jr C R. Study of the solid/liquid interface during unidirectional solidification of cast iron. Transactions of the American Foundrymen's Society, 1990, 98: 483–488.
[8] Holmgren D. Review of thermal conductivity of cast iron. International Journal of Cast Metals Research, 2005, 18(6): 331–345.
[9] Chen G. Nanoscale energy transport and conversion. MIT-Pappalardo Series in Mechanical Engineering, Oxford University Press, 2005.
[10] Wang G H, Li Y X. Effects of alloying elements and temperature on thermal conductivity of ferrite. Journal of Applied Physics, 2019, 126(12): 125118.
[11] Tritt T M. Thermal conductivity: theory, properties, and applications. Springer Science & Business Media, 2005.
[12] Holmgren D, Diszegi A, Svensson I L, et al. Effects of nodularity on thermal conductivity of cast iron. International Journal of Cast Metals Research, 2007, 20(1): 30–40.
[13] Holmgren D, Selin M. Regression model describing the thermal conductivity of various cast irons. Materials Science Forum, 2010, 649: 499–504.
[14] Selin M, Konig M. Regression analysis of thermal conductivity based on measurements of compacted graphite irons. Metallurgical and Materials Transactions A - Physical Metallurgy and Materials Science, 2009, 40A: 3235–3244.
[15] Jalava K, Soivio K, Laine J, et al. Effect of silicon and microstructure on spheroidal graphite cast iron thermal conductivity at elevated temperatures. International Journal of Metalcasting, 2017, 7: 1–7.

[16] Wang G Q, Chen X, Li Y X. Fuzzy neural network analysis on the gray cast iron with high thermal conductivity and tensile strength. China Foundry, 2019, 16(3): 190–197.
[17] Helsing J, Helte A. Effective conductivity of aggregates of anisotropic grains. Journal of Applied Physics, 1991, 69(6): 3583–3588.
[18] Helsing J, Grimvall G. Thermal conductivity of cast iron: Models and analysis of experiments. Journal of Applied Physics, 1991, 70(3): 1198–1206.
[19] Nan C W, Birringer R, Gleiter H, et al. Effective thermal conductivity of particulate composites with interfacial thermal resistance. Journal of Applied Physics, 1997, 81(10): 6692–6699.
[20] Velichko A, Wiegmann A, Mücklich F. Estimation of the effective conductivities of complex cast iron microstructures using FIB-tomographic analysis. Acta Materialia, 2009, 57(17): 5023–5035.
[21] Ma Z J, Wen Q, Tao D, et al. Numerical simulation and analysis of thermal conductivity of vermicular graphite cast iron. Journal of Xi'an Technological University, 2016, 36: 522–527. (In Chinese)
[22] American Society for Testing and Materials. Standard test method for steady-state thermal transmission properties by means of the heat flow meter apparatus. ASTM International, 2017.
[23] Li L B, Sun Y F. Handbook of physical properties of metal materials. China Machine Press, 2011: 96–104. (In Chinese)
[24] Kai M, Bin L, Guang W. Application of measuring method of thermal conductivities. Storage and Process, 2005, 5(6): 35–38.
[25] Stalhane B, Pyk S. New method for determining the coefficients of thermal conductivity. Tek. Tidskr, 1931, 61(28): 389–393.
[26] Gustafsson S E. Transient plane source techniques for thermal conductivity and thermal diffusivity measurements of solid materials. Review of Scientific Instruments, 1991, 62(3): 797–804.
[27] Parker W J, Jenkins R J, Butler C P, et al. Flash method of determining thermal diffusivity, heat capacity, and thermal conductivity. Journal of Applied Physics, 1961, 32(9): 1679–1684.
[28] Xu D M, Wang G Q, Chen X, et al. Effects of alloy elements on ductility and thermal conductivity of compacted graphite iron. China Foundry, 2018, 15(3): 189–195.
[29] Dawson S. Compacted graphite iron: mechanical and physical properties for engine design. Vdi Berichte, 1999, 1472: 85–106.
[30] Maxwell J C. A treatise on electricity and magnetism. Oxford: Clarendon Press, 1873.
[31] Eucken A. General regulations for the thermal conductivity of different types of substances and aggregate states. Research in the Field of Engineering A, 1940, 11(1): 6–20. (In German)
[32] Xu J Z, Gao B Z, Kang F Y. A reconstruction of Maxwell model for effective thermal conductivity of composite materials. Applied Thermal Engineering, 2016, 102: 972–979.
[33] Bruggeman V D A G. Calculation of various physics constants in heterogenous substances, I: Dielectricity constants and conductivity of mixed bodies from isotropic substances. Annals of Physics, 1935, 416(7): 636–664. (In German)
[34] Nan C W, Birringer R, Clarke D R, et al. Effective thermal conductivity of particulate composites with interfacial thermal resistance. Journal of Applied Physics, 1997, 81(10): 6692–6699.
[35] Hasselman D P H, Johnson L F. Effective thermal conductivity of composites with interfacial thermal barrier resistance. Journal of Composite Materials, 1987, 21(6): 508–515.
[36] Hamilton R L, Crosser O K. Thermal conductivity of heterogeneous two-component systems. Industrial & Engineering Chemistry Fundamentals, 1962, 1(3): 187–191.
[37] Hatta H, Taya M, Kulacki F A, et al. Thermal diffusivities of composites with various types of filler. Journal of Composite Materials, 1992, 26(5): 612–625.
[38] Holmgren D M, DiÃszegi A, Svensson I L, et al. Effects of transition from lamellar to compacted graphite on thermal conductivity of cast iron. Cast Metals, 2006, 19(6): 303–313.
[39] Liu Y Z, Li Y F, Xing J D, et al. Effect of graphite morphology on the tensile strength and thermal conductivity of cast iron. Materials Characterization, 2018, 144: 155–165.
[40] Matsushita T, Saro A G, Elmquist L, et al. On the thermal conductivity of CGI and SGI cast irons. International Journal of Cast Metals Research, 2018, 31(3): 135-143.
[41] Hashin Z, Shtrikman S. A variational approach to the theory of the effective magnetic permeability of multiphase materials. Journal of Applied Physics, 1962, 33(10): 3125–3131.
[42] Fredriksson H, Svensson I L. Computer simulation of the structure formed during solidification of cast iron. MRS Proceedings, 1984, 34: 273.
[43] Dardati P M, Godoy L A, Celentano D J. Microstructural simulation of solidification process of spheroidal-graphite cast iron. Journal of Applied Mechanics, 2006, 73(6): 977–983.
[44] Sun Y, Luo J, Mi G F, et al. Numerical simulation and defect elimination in the casting of truck rear axle using a nodular cast iron. Materials & Design, 2011, 32(3): 1623–1629.
[45] Yin Y J, Tu Z X, Shen X, et al. Digitizing casting techology of nodular iron. Modern Cast Iron, 2018, 38(05): 63–68. (In Chinese)
[46] Fukumasu N K, Pelegrino P L, Cueva G, et al. Numerical analysis of the stresses developed during the sliding of a cylinder over compact graphite iron. Wear, 2005, 259: 1400–1407.
[47] Tkaya M B, Mezlini S, Mansori M E, et al. On some tribological effects of graphite nodules in wear mechanism of SG cast iron: Finite element and experimental analysis. Wear, 2009, 267(1): 535–539.
[48] Ljustina G, Larsson R, Fagerström M. A FE based machining simulation methodology accounting for cast iron microstructure. Finite Elements in Analysis and Design, 2014, 80: 1–10.
[49] Velichko A, Holzapfel C, Muecklich F. 3D characterization of graphite morphologies in cast iron. Advanced Engineering Materials, 2007, 9: 39–45.
[50] Swartz E T, Pohl R O. Thermal boundary resistance. Reviews of Modern Physics, 1989, 61(3): 605.
[51] Stoner R J, Maris H J. Kapitza conductance and heat flow between solids at temperatures from 50 to 300 K. Physical Review B: Condensed Matter, 1993, 48(22): 16373.
[52] Yang W, Ma Z J, Yang Z, et al. Numerical simulation of the effect of oxidation on the thermal conductivity of vermicular graphite cast iron. Journal of Xi'an Technological University, 2019, 39: 458–462. (In Chinese)
[53] Selin M. Using regression analysis to optimize the combination of thermal conductivity and hardness in compacted graphite iron. Key Engineering Materials, 2010, 457: 337–342.
[54] Selin M. Tensile and thermal properties in compacted graphite irons at elevated temperatures. Metallurgical and Materials Transactions A, 2010, 41(12): 3100–3109.
[55] Williams R K, Yarbrough D W, Masey J W, et al. Experimental determination of the phonon and electron components of the thermal conductivity of bcc iron. Journal of Applied Physics, 1981, 52(8): 5167–5175.
[56] Williams R K, Graves R S, Weaver F J, et al. Effect of point defects on the phonon thermal conductivity of bcc iron. Journal of Applied Physics, 1987, 62(7): 2778–2783.
[57] Terada Y, Ohkubo K, Mohri T, et al. Effects of alloying additions on thermal conductivity of ferritic iron. ISIJ international, 2002, 42(3): 322–324.

[58] Rukadikar M C, Reddy G P. Influence of chemical composition and microstructure on thermal conductivity of alloyed pearlitic flake graphite cast irons. Journal of Materials Science, 1986, 21(12): 4403–4410.
[59] Donaldson J W. The thermal conductivities of high-duty and alloy cast irons. British Foundryman, 1938, 32: 125–131.
[60] Ding X F, Li X Z, Huang H, et al. Effect of Mo addition on as-cast microstructures and properties of grey cast irons. Materials Science and Engineering: A, 2018, 718: 483–491.
[61] Xu D M, Wang G Q, Chen X, et al. Effects of Mo and Ni on the thermal conductivity of compacted graphite iron at elevated temperature. International Journal of Cast Metals Research, 2019: 1–9.
[62] Korn D, Pfeifle D P H, Niebuhr J. Electrical resistivity of metastable copper-iron solid solutions. Zeitschrift Für Physik B Condensed Matter, 1976, 23(1): 23–26.
[63] Angus H T. Mechanical, physical and electrical properties of cast iron. Cast Iron Physical & Engineering Properties, 1976, 48(2): 34–160.
[64] Ho C Y, Powell R W, Liley P E. Thermal conductivity of the elements. Journal of Physical and Chemical Reference Data, 1972, 1(2): 279–421.
[65] Haynes W M. CRC Handbook of Chemistry and Physics, 97th Edition. Taylor & Francis Group, London, New York, 2017: 2117–2295.
[66] Pehlke R D, Jeyarajan A, Wada H. Summary of thermal properties for casting alloys and mold materials. NASA STI/Recon Technical Report N, 1982, 83.
[67] Balandin A A. Thermal properties of graphene and nanostructured carbon materials. Nature Materials, 2011, 10(8): 569–581.
[68] Klemens P G, Pedraza D F. Thermal conductivity of graphite in the basal plane. Carbon, 1994, 32(4): 735–741.
[69] Gorny M, Lelito J, Kawalec M, et al. Thermal conductivity of thin walled compacted graphite iron castings. ISIJ International, 2015, 55(9): 1925–1931.
[70] Holmgren D, Källbom R, Svensson I L. Influences of the graphite growth direction on the thermal conductivity of cast iron. Metallurgical and Materials Transactions A, 2007, 38(2): 268–275.
[71] Buning K D, Taran U N. Cast iron structure. China Machine Press, 1977. (In Chinese)
[72] Lux B, Minkoff I, Mollard F, et al. Branching of graphite crystals growing from a metallic solution. In: Proc. 2nd Internat. Symposium on The Metallurgy of Cast Iron, 1976: 495–508.
[73] Ruff G F, Wallace J F. Graphite configuration in gray iron. American Foundrymen's Society, 1977 AFS Research Reports, 1978: 11–14.
[74] Liu B C, et al. Study on morphology of vermicular graphite. Modern Cast Iron, 1982, (4): 8–11. (In Chinese)
[75] Li C L, Liu B C, Wu D H. Graphite atlas of cast iron: photographs of optics and scanning electron microscope. China Machine Press, 1983. (In Chinese)
[76] Velichko A, Holzapfel C, Siefers A, et al. Unambiguous classification of complex microstructures by their three-dimensional parameters applied to graphite in cast iron. Acta Materialia, 2008, 56(9): 1981–1990.
[77] Yang Z, Wang J W, Feng Y P, et al. Crystallization kinetics of eutectic gray cast iron. Transactions of Materials and Heat Treatment, 2017, 38: 152–158.
[78] Fan H Y, et al. The influence of temperature on the thermal conductivity of cast irons. Materials Review, 1996, 3: 23–25. (In Chinese)
[79] Peet M J, et al. Prediction of thermal conductivity of steel. International Journal of Heat and Mass Transfer, 2011, 54(11-12): 2602–2608.
[80] Williams R K, Graves R S, Mcelroy D L. Thermal and electrical conductivities of an improved 9 Cr-1 Mo steel from 360 to 1000 K. International Journal of Thermophysics, 1984, 5(3): 301–313.
[81] Julian C L. Theory of heat conduction in rare-gas crystals. Physical Review, 1965, 137(1A): 128–137.
[82] Klemens P G. Theory of the a-plane thermal conductivity of graphite. Journal of Wide Bandgap Materials, 2000, 7(4): 332–339.
[83] Zhou J Y. Colour metallography of cast iron. China foundry, 2009, 6(1): 57–69.
[84] Wang G Q, Chen X, Li Y X, et al. Effects of alloying elements on thermal conductivity of pearlitic gray cast iron. Journal of Iron and Steel Research International, 2019, 26(9): 1022–1030.
[85] Wang G Q, Chen X, Li Y X, et al. Effects of inoculation on the pearlitic gray cast iron with high thermal conductivity and tensile strength. Materials, 2018, 11(10): 1876.